JOURNAL OF MAGNETIC RESONANCE **125,** 280–290 (1997)
ARTICLE NO. MN971108

Search for a Magnetic-Field Dependence of the Interaction of the Nuclear Quadrupole Moment with the Electric-Field Gradient

B. FILSINGER,* P. GUTSCHE,* U. HAEBERLEN,* AND N. WEIDEN†

*Max-Planck-Institut für Medizinische Forschung, Jahnstraße 29, 69120 Heidelberg, Germany; and †Institut für Phys. Chemie, Technische Hochschule Darmstadt, Petersenstraße 20, 64287 Darmstadt, Germany

Received November 4, 1996; revised December 18, 1996

It is argued that the nuclear quadrupole–electric field gradient (EFG) interaction is, in principle, dependent on the presence of a magnetic field B. A rough estimate of the size of this effect yields 10^{-4} in fields up to 10 T. However, if the site symmetry of the nucleus in question includes time-reversal symmetry, the linear dependence of the EFG on B vanishes. In diamagnetic compounds, time-reversal symmetry is violated only by the presence of nuclear spins. In such compounds, the dominant dependence of the EFG on B should be quadratic and should be described by a fourth-rank tensor. In ferro- and antiferromagnetic compounds time-reversal symmetry is strongly violated and a linear dependence of the EFG on B, described by a third-rank tensor, is expected. A search for a magnetic field dependence of the EFG was carried out by measuring the quadrupole coupling constants (QCCs) of the ^{27}Al and ^{14}N nuclei in corundum and sodium nitroprusside (SNP) by pure NQR, and by NMR in fields of 6.3 and 11 T. These diamagnetic compounds were selected because previous measurements, done in different fields, yielded differing results for the QCCs. A new technique for measuring QCCs by NMR is introduced that circumvents the necessity of precisely orienting the sample crystals. For the QCCs of both the ^{27}Al and ^{14}N nuclei in corundum and SNP, respectively, a precision of distinctly better than 10^{-4} is reached. The results obtained in 0, 6.3, and 11 T fields fully agree with each other which means that, in fields up to 11 T, any possible field dependence of the QCCs is smaller than 10^{-4}. These results confirm that in diamagnetic compounds a linear dependence of QCCs on B is largely suppressed. © 1997 Academic Press

INTRODUCTION

Quadrupole coupling, that is, the interaction of the quadrupole moment eQ of a nucleus with the electric field gradient (EFG) at the nuclear site, plays a major role in many areas of solid-state physics. It is the basis of nuclear quadrupole resonance spectroscopy, and in solid-state nuclear magnetic resonance of $I > \frac{1}{2}$ nuclei, it usually plays the dominant role next to the Zeeman interaction.

The EFG is the second derivative, taken at the nuclear site, of the electric potential $V(\mathbf{x})$

$$V_{ij} = \frac{\partial^2 V(\mathbf{x})}{\partial i \partial j},\ i, j = x, y, z. \qquad [1]$$

Since this potential is determined by the surroundings of the nucleus on a microscopic scale, the EFG provides information about the structure of the surroundings, e.g., about the direction and length of a chemical bond. Therefore, the determination of EFGs is one of the most often undertaken tasks in NQR and in solid-state NMR.

It is generally assumed that the EFG is independent of the presence or absence of a magnetic field **B**. Intuition, however, tells us that a dependence of the EFG on a magnetic field should exist: The presence of a magnetic field modifies the electronic wavefunction and thus the charge distribution of a molecule. If it did not, we would not observe chemical shifts. Because the electronic charge distribution in a molecule or crystal, together with the nuclear point charges, determines the EFG sensed by a nucleus, a magnetic-field-induced modification of the electronic wavefunction must also lead to a modified EFG

$$V_{ij}(\mathbf{B}) = V_{ij}(\mathbf{B} = 0) + \Delta V_{ij}(\mathbf{B}). \qquad [2]$$

Henceforth, a nonzero modification $\Delta V_{ij}(\mathbf{B})$ of the EFG will be called the *effect.* The search for the *effect* is the subject of this paper. We may also argue that there is no general law prohibiting a magnetic field dependence of the EFG and that, therefore, the *effect* should exist.

The well-known phenomenon of magnetostriction, which is trivially accompanied by a field dependence of the EFG at nuclear sites, is proof that a general law prohibiting the effect indeed cannot exist. Magnetostriction is observed in materials with ordered electronic spins, e.g., in crystals of nickel and iron (*1*). In what follows, we shall not be concerned with such systems. Instead, we ask whether an effect may also be observed in diamagnetic materials.

While the arguments for the existence of the effect are, we think, convincing, the crucial question is, of course, how large will it be. Before embarking on experiments, both an

1090-7807/97 $25.00

estimate of the size of the effect and a literature search for data which possibly imply an already observed effect are therefore in order.

First, let us assume that an effect with a linear dependence of the EFG on **B** exists. Then, using first-order perturbation theory, one may arrive at the estimate

$$\frac{\Delta V_{ij}}{V^{o}_{ij}} \sim \frac{|\mathbf{B}| \cdot \mu_{\mathrm{Bohr}}}{E_B}, \qquad [3]$$

where $V^{o}_{ij} := V_{ij}(\mathbf{B} = 0)$ and E_B is a ''typical'' electronic excitation energy. With $|\mathbf{B}| = 10$ T (a typical field used in NMR) and $E_B = 10$ eV, Eq. [3] ''predicts'' an effect on the order of 10^{-4}. An effect of this size would be detectable with the measurements described in this paper under Experimental. A more careful application of perturbation theory leads, however, to the conclusion that orbital quenching (*2*) suppresses a linear effect to a large extent (*3*). We shall demonstrate under Phenomenology that no linear (in general: no odd-order) effect should exist at all if the sample crystal obeys time-reversal symmetry. In diamagnetic crystals, time-reversal symmetry is violated only by the presence of the nuclear spins, i.e., it is violated only extremely weakly. Therefore, it does not come as a surprise that at the present level of precision of our experiments we could not find convincing evidence for an effect in diamagnetic systems.

We now turn to possible hints for the effect in already published data. An extensive literature search revealed that quadrupole coupling constants QCC measured by NQR (i.e., in the absence of an applied magnetic field) and by NMR (i.e., in the presence of a large magnetic field) often deviate from each other by a margin which is larger than the combined quoted error limits. Note that the quadrupole coupling constant, QCC $= e^2qQ/h$, is proportional to the largest principal component, eq, of the EFG tensor. The comparison of published NQR and NMR data is, however, usually hampered by the fact that the measurements were carried out at different temperatures. A notable exception is sodium nitroprusside (SNP), $Na_2[Fe(CN)_5NO] \cdot 2H_2O$. Using NMR with $|\mathbf{B}| = 8.35$ T, Gross *et al.* measured at room temperature the four distinct ^{14}N quadrupole coupling tensors in SNP (*4*). The QCCs derived from these data are listed in the first column of Table 1. Subsequently, Murgich *et al.* measured by NQR the temperature dependence of the ^{14}N QCCs in SNP (*5*). Their room-temperature results are listed in the second column of Table 1, and the third column shows the differences between the NMR and NQR results. These differences are definitely larger than the combined error limits of the two experiments. We discussed the discrepancy with Murgich, but neither group could locate a flaw in its measurements and the data analysis. What remained as an explanation was the presence or absence of a magnetic field in the NMR and NQR measurements, and thus a hint of the effect.

TABLE 1

Literature Values of the Quadrupole Coupling Constants of the Four Distinct Nitrogens in SNP, $Na_2[Fe(CN)_5NO] \cdot 2H_2O$ at Room Temperature

Site	QCC/kHz from NMR (*4*)	QCC/kHz from NQR (*5*)	Difference (kHz)
N0	2239	2237	+2
N1	3560	3569	−9
N2	3489	3515	−26
N3	3635	3657	−22

Note. The labeling of the sites follows Fig. 2. The NMR data are from measurements in a field of 8.35 T. The NQR values were extracted from Fig. 2 of Ref. (*5*).

In our search for the effect, we therefore went back to the ^{14}N nuclei in SNP, repeating the NQR measurements of the four distinct QCCs and performing new NMR measurements at 6.3 and 11.0 T. The latter experiments were designed in such a way that the QCCs obtained are free from uncertainties of the crystal orientation. As shown below under Experimental, we must state that no effect was found and that both Gross *et al.* and Murgich *et al.* had overestimated the accuracy of their measurements.

The ^{14}N atoms in SNP are predominantly bonded covalently (—C≡N and —N═O). To extend the search for the effect to an ionic bonding situation, we also studied the ^{27}Al nuclei in corundum, α-Al_2O_3. Since the very early days of NMR and NQR, corundum has been a favorite compound for demonstrating new experimental methods applicable to half-integer quadrupolar nuclei. Values for the QCC of ^{27}Al in corundum were reported by Pound (*6*), Chang *et al.* (*7*), Jakobsen *et al.* (*8*), and Gravina *et al.* (*9*). In Fig. 1, we show these data together with their error limits. We present them on a temperature axis together with our own measurements to stress the importance of temperature in comparisons of QCCs reported by different authors. The present data were collected at $|\mathbf{B}| = 11$ T, whereas the published data were recorded in different fields that are given in the legend of Fig. 1. Obviously, there are discrepancies outside the quoted error limits, and obviously the discrepancies cannot be attributed to different temperatures. Once again, these discrepancies may reflect a magnetic field dependence of the QCC, and once again, the results of this paper will demonstrate that within the error limits of our own measurements, which are much smaller than those of previous workers, there is no magnetic field dependence of the QCC in corundum.

PHENOMENOLOGY OF THE EFFECT

General

For the phenomenological description of the effect, we expand the components V_{ij} of the EFG with respect to the components B_k of the applied field, that is,

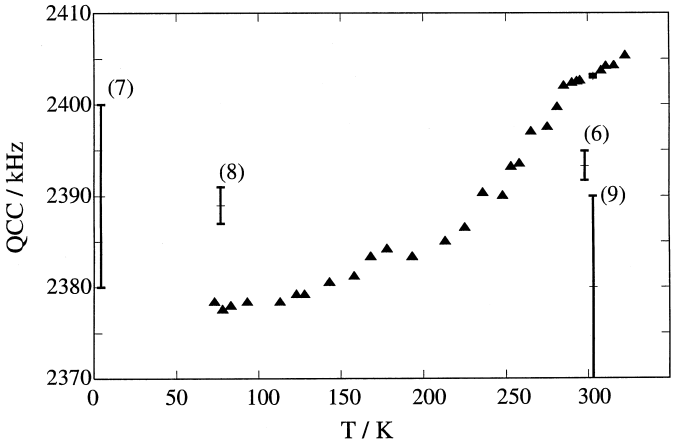

FIG. 1. Temperature dependence of the quadrupole coupling constant QCC of ^{27}Al in corundum, α-Al_2O_3 (▲), and literature values (with errorbars). The data from this work were collected in a field of 11 T; the values from Refs. (*6, 8*) were obtained in fields of 0.24 and 9.4 T, respectively, whereas those of Refs. (*7, 9*) were obtained in a zero magnetic field.

$$V_{ij}(\mathbf{B}) = V^{o}_{ij} + \frac{\partial V_{ij}}{\partial B_k} B_k + \frac{1}{2} \frac{\partial^2 V_{ij}}{\partial B_k \partial B_l} B_k B_l + \cdots . \quad [4]$$

The usual summation rule is implied for the indices i, j, k, and l. Restricting ourselves to the first- and second-order terms of the expansion, we rewrite Eq. [4] as

$$V_{ij}(\mathbf{B}) = V^{o}_{ij} + V_{ijk} B_k + V_{ijkl} B_k B_l . \quad [5]$$

The terms $V_{ijk}B_k$ and $V_{ijkl}B_kB_l$ describe, respectively, the *linear* and the *quadratic effects,* i.e., the linear and the quadratic dependences of the EFG on $\mathbf{B}$.

V^{o}_{ij} is a second-rank polar tensor, as must be $V_{ij}(\mathbf{B})$. Therefore, V_{ijk} is a pseudo tensor of third rank, and V_{ijkl} is a polar tensor of fourth rank. All these tensors are *microscopic* tensors, defined and therefore fixed at a particular nuclear site. They result from a particular nuclear environment and represent microscopic properties of the crystal. Hence, they must be invariant under the symmetry operations of this nuclear site. The important consequences of this invariance will be discussed in the next two sections.

For the moment, we note the *intrinsic* symmetry of these tensors. The interchangeable order of the derivatives in Eq. [4] allows the positions of the indices i, j of all tensor components in Eq. [5] as well as the positions of the indices k, l in V_{ijkl}, to be interchanged. This consideration restricts the tensors V^{o}_{ij}, V_{ijk}, and V_{ijkl} to have, respectively, 6, 18, and 36 independent components.

Spatial Site Symmetry

All tensors in Eq. [4] must be invariant under the operations of the elements of the point group of the *site symmetry.* The site symmetry of the ^{27}Al nuclei in α-Al_2O_3 is 3 (*10*). This implies that V^{o}_{ij} is axially symmetric, i.e., its asymmetry factor η must be zero, a fact that has been overlooked even in very recent work (*8, 9*), and that its symmetry axis coincides with the threefold axis of the crystal. Moreover, it reduces the number of independent components of V_{ijk} from 18 to 6 and that of V_{ijkl} from 36 to 12 (*13*). In SNP, the nitrogens N1 and N0 lie in a symmetry plane. As a consequence, the number of independent components of V^{o}_{ij}, V_{ijk}, and V_{ijkl} is reduced from 6 to 4, 18 to 10, and 36 to 20, respectively. The nitrogens N2 and N3 occupy general sites and no simplification of site-attached tensors results. The labeling of the nitrogens in SNP is defined in Fig. 2.

Site Symmetry with Respect to Time Reversal

An operation belongs to the group $\mathcal{G}$ of symmetry operations of the *site symmetry* if it leaves invariant the microscopic environment of the site in the crystal. If this environment is completely described by the probability density of all nuclei and electrons, $|\Psi(\mathbf{x}_n, \mathbf{x}_e)|^2$, then the antiunitary, antilinear time-reversal operation $\mathbf{T}$ leads to

$$|\mathbf{T}\Psi(\mathbf{x}_n, \mathbf{x}_e)|^2 = |(\mathbf{T}\Psi)^*\mathbf{T}\Psi| = |\Psi\Psi^*| = |\Psi(\mathbf{x}_n, \mathbf{x}_e)|^2 \quad [6]$$

because $\mathbf{T}\Psi = \Psi^*$. In this case, $\mathbf{T}$ *is* an element of $\mathcal{G}$. The situation is different if, for the complete description of the environment, one must also consider nonvanishing angular momenta $\mathbf{J}$, because $\mathbf{TJ} = -\mathbf{J}$.

If we disregard nuclear spins for the moment, the former situation is realized in diamagnetic crystals such as corundum and SNP, while the latter applies to ferro-, antiferro-, and ferrimagnetic systems (paramagnetic crystals require special consideration, as shown below). Now, from $\mathbf{TB} = -\mathbf{B}$ and the definition of the tensors in Eq. [5], it follows that

$$\begin{aligned} \mathbf{T}V^{o}_{ij} &= V^{o}_{ij} \\ \mathbf{T}V_{ijk} &= -V_{ijk} \\ \mathbf{T}V_{ijkl} &= V_{ijkl} . \end{aligned} \quad [7]$$

Still disregarding nuclear spins, we conclude that the linear effect, described by V_{ijk}, should vanish in diamagnetic compounds such as corundum and SNP. By contrast, in ferro-, ferri-, and antiferromagnetic crystals, V_{ijk} will not vanish in general. As already mentioned in the Introduction, in such crystals the EFG is expected to depend on $\mathbf{B}$, and we may now add that the dependence will include a term linear in $\mathbf{B}$.

Let us briefly consider paramagnetic compounds. Macroscopically, they are invariant under $\mathbf{T}$ because the operation leads from one disordered (spin) state to another, indistinguishable from the former on a macroscopic scale. On a

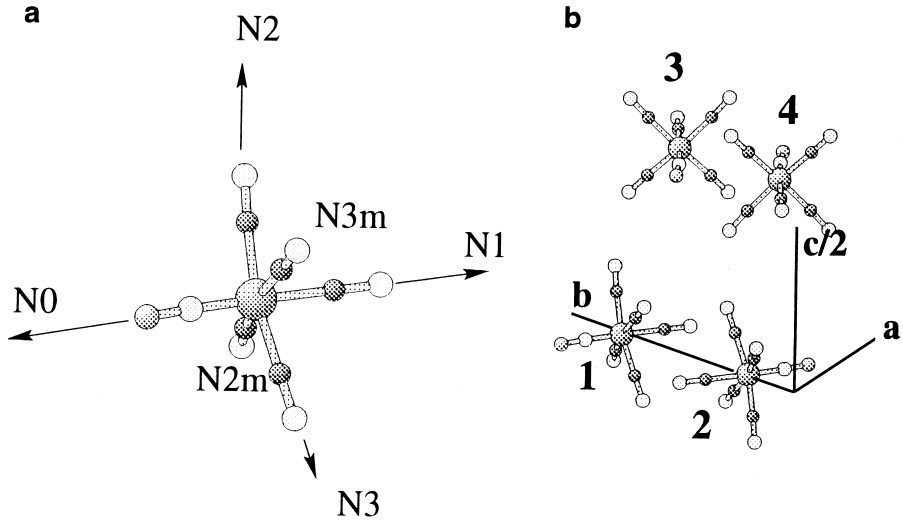

FIG. 2. (a) The $Fe(CN)_5NO$ complex of SNP. (b) The arrangement of the four $Fe(CN)_5NO$ complexes in the unit cell. The *ab* plane is a mirror plane of the crystal. The Fe atom and the N, O, and C atoms of the N0 and N1 groups all lie in this mirror plane.

microscopic scale, the situation is different. Locally, the inversion of the spin orientations leads to a different environment of a site and V_{ijk} is, therefore, not necessarily zero. It will vary from one nuclear site to the next and therefore lead to an inhomogeneous interaction and eventually to an inhomogeneous line broadening. This broadening, however, is subject to motional averaging due to mutual dipole–dipole interactions, if the spins are flipping or have short spin–lattice relaxation times. What we have said in this paragraph applies primarily to electronic, but in principle also to nuclear spins. However, the violation of time-reversal symmetry by the presence of the nuclear spins in diamagnetic compounds may be expected to have such a tiny influence upon the effect, which anyhow is small, that it may be safely disregarded. Before concluding this discussion, we briefly mention that the very application of a magnetic field, indispensable in any search for the effect, will also *lower* the site symmetry (*12*) and thus lead to a secondary effect which, however, will be much weaker than the primary effect (*13*).

Strategies for Detecting the Effect

We divide the task into two parts. First, we ask what is the best way to detect the overall effect. Then we discuss how individual components of V_{ijk} and V_{ijkl} can be measured.

The most natural way of searching for the overall effect is to measure by NMR, at different strengths of the applied field $\mathbf{B}$, the quadrupole coupling tensor $Q_{ij} = 3e\mathrm{Q}\mathrm{V}_{ij}/2Ih$ of the nucleus of interest and to look for differences of its largest component $Q_{ZZ}(\mathbf{B}) = 3e\mathrm{Q}\mathrm{V}_{ZZ}(\mathbf{B})/2Ih$. It is, of course, advisable to include in this search the largest available field, and also to measure the quadrupole coupling constant $QCC(\mathbf{B} = 0) = eQV^{\circ}_{ZZ}/h$ by pure NQR. For distinguishing a *linear* from a *quadratic effect*, it is obviously necessary to measure $Q_{ZZ}(\mathbf{B})$ by NMR for at least two different strengths of the applied field. Naturally, we used fields of 6.3 and 11 T, available in our laboratory, to search for the effect in corundum and SNP.

The standard way of measuring a quadrupole coupling tensor Q_{ij} by high-field NMR is to rotate a crystal about two nonorthogonal (*11*) or three orthogonal axes in a goniometer whose axis is perpendicular to the applied field $\mathbf{B}$, and to record, for each rotation axis $\mathbf{R}^{(i)}$, a *rotation pattern* of *satellite* splittings $\Delta\nu^{(i)}(\varphi)$, where φ is the rotation angle. For the $I = \frac{5}{2}$ nuclei ^{27}Al, we take the splitting of the *outer* satellites. From such a set of data, the complete tensor Q_{ij} can be evaluated, including the largest principal component Q_{ZZ} and the direction of the associated principal axis, $\mathbf{e}_Z$.

The drawback of this procedure is that it hinges on precisely orienting a crystal, on precisely setting rotation angles, and on a perfect alignment of the goniometer axis perpendicular to the applied field. These are actually the problems which usually limit the accuracy of a quadrupole-coupling-tensor determination by the standard procedure.

To circumvent these problems in our search for the effect, we chose a different approach. Both for the ^{27}Al nuclei in corundum and for the ^{14}N nuclei in SNP, we know the direction of the principal axis $\mathbf{e}_Z$, either by crystal symmetry (corundum) or by previous measurements (*4*). Since this direction $\mathbf{e}_Z$ is of central importance to our approach, we term it the *pole of the tensor.*

Our procedure of measuring Q_{ZZ} is to search on a two-dimensional grid, with $\mathbf{B}$ in the neighborhood of the pole, for the largest value of $\Delta\nu$. This method relies on the fact that $\Delta\nu$ assumes a global maximum when $\mathbf{B}$ is exactly at the pole. To this end, we built an NMR probe that allows us to tilt the axis of a standard NMR goniometer up to $\pm 3°$

in a controlled manner about an axis perpendicular to **B**. Using this probe, the splitting $\Delta\nu$ becomes a function of both the rotation angle φ and the tilt angle ψ. The task of orienting crystals is reduced to ensuring that a desired pole direction $\mathbf{e}_Z$ can be made parallel to **B** by using both the rotation and tilt movements. We know we have fulfilled this task if $\Delta\nu(\varphi, \psi)$ goes through a maximum somewhere within the range $-3° < \psi < 3°$ for some arbitrary angle φ. The maximum value itself gives $Q_{ZZ}(\mathbf{B})$ and, eventually, $V_{ZZ}(\mathbf{B})$. Together with NQR measurements of V^o_{ZZ}, this procedure gives the tensor components V_{ZZZ} and V_{ZZZZ}, provided that the error limits are small enough. Details are described under Experimental and Results.

We proceed by commenting briefly on how to access other components of V_{ijk} and V_{ijkl}. Of course, we need additional measurements. An obvious possibility is to record rotation patterns $\Delta\nu^{(i)}(\varphi)$. Let us assume we know how to adjust the rotation axis of the goniometer exactly perpendicular to **B**, a tricky task of its own. In the absence of an effect and relying on first-order perturbation theory, the functional form of $\Delta\nu^{(i)}(\varphi)$ is (*14*)

$$\Delta\nu^{(i)}(\varphi) = c^{(i)} + a^{(i)}\cos 2\varphi + b^{(i)}\sin 2\varphi \qquad [8]$$

for an arbitrary rotation axis $\mathbf{R}^{(i)}$ where $c^{(i)}$, $a^{(i)}$, and $b^{(i)}$ are linear combinations of the components of V^o_{ij} with known coefficients that depend on $\mathbf{R}^{(i)}$. Now, let us impose the effect. To simplify the notation, we drop the index i from now on. The functional form of $\Delta\nu(\varphi)$ becomes

$$\begin{aligned}\Delta\nu(\varphi) = {} & c + a\cdot\cos 2\varphi + b\cdot\sin 2\varphi \\ & + A_1\cos\varphi + B_1\sin\varphi + A_3\cos 3\varphi + B_3\sin 3\varphi \\ & + C_2 + A_2\cos 2\varphi + B_2\sin 2\varphi \\ & + A_4\cos 4\varphi + B_4\sin 4\varphi, \end{aligned} \qquad [9]$$

where A_1, B_1, A_3, B_3 and C_2, A_2, B_2, A_4, and B_4 are linear combinations of the components of V_{ijk} and V_{ijkl}, respectively. The coefficients $(c + C_2)$, A_1, $(a + A_2)$, . . . , B_4 can be extracted from the rotation pattern by Fourier analysis. At least for simple cases like ^{27}Al in corundum, in which V^o_{ij} is axially symmetric because of crystal symmetry, the coefficients c, a, b (and other ones if first-order perturbation theory is insufficient) are available from an NQR measurement. Therefore, we can say that the Fourier analysis of $\Delta\nu(\varphi)$ yields A_1, B_1, . . . , A_4, B_4. Note that for every rotation axis $\mathbf{R}^{(i)}$ there is a separate set of such coefficients, which can be used to calculate the components of V_{ijk} and V_{ijkl}. However, not all components of these tensors are accessible in this way. Of the 6 independent components of V_{ijk} and 12 of V_{ijkl} in corundum, only 5 and 11, respectively, are accessible (*13*). This means that some of the components of these tensors represent *longitudinal*, others *transverse* effects (*15*). The second-rank chemical-shift tensor is an analogous example: its symmetric part causes longitudinal effects while the antisymmetric part causes transverse effects. Indeed, only the components of the former lead to *line shifts*, which are directly proportional to these components (*16*).

EXPERIMENTAL AND RESULTS

Samples

For the ^{27}Al NMR and NQR measurements in corundum, two oriented cylindrical crystals of synthesized α-Al_2O_3 were purchased from Wiede's Carbidwerk in Freyung. The NMR crystal had a length of 12 mm and a diameter of 5 mm. The corresponding dimensions of the NQR crystal were 50 and 21 mm. For both crystals, we specified that the crystallographic c axis be perpendicular to the cylinder axis and, according to the manufacturer, it *is* within $\pm 2°$. Note, first, that for the NMR crystal, the pole of the ^{27}Al EFG tensor can be rotated with our NMR goniometer into an orientation parallel to the applied field and that the tilt mechanism of the probe can take care of the tolerance of $\pm 2°$. Note, second, that a powder sample would have been sufficient for the NQR measurements. It would have meant, however, a sacrifice of sensitivity which we wanted to avoid in view of the anticipated difficulties of observing the ^{27}Al NQR in corundum at room temperature, as discussed below. Remember that the NQR crystal is oriented in such a way that the exciting RF field $\mathbf{B}_1$, which is parallel to the cylinder axis, is perpendicular to the ^{27}Al tensor pole, that is, $\mathbf{B}_1$ is along the direction which gives the maximum NQR sensitivity.

For the ^{14}N NMR and NQR measurements in SNP, three large pieces of oriented single crystals were kindly given us by S. Haussühl. Two of them were used to prepare two cylindrical NMR samples (diameter 11 mm, length 10 mm) for the EFG tensor pole measurements. To understand the direction of the respective cylinder axis which we chose for these samples, it is necessary to look at the structure of SNP, the important aspects of which are shown in Fig. 2. The space group of SNP is *Pnnm* with $Z = 4$ (*17*). The $Fe(CN)_5NO$ complexes labeled 1 and 2, and 3 and 4 in Fig. 2b are related by inversion centers and are thus magnetically equivalent. The complexes 1 and 3, and 2 and 4 are related by twofold screw axes and therefore are crystallographically equivalent. The *ab* plane of the crystal is a mirror plane, which relates the nitrogens N2 and N2m, and N3 and N3m. The nitrogens N0 and N1 lie in that plane, as do their bonds. According to (*4*), the principal EFG direction $\mathbf{e}_Z$, that is, the EFG *pole* of every nitrogen in SNP is very close to the respective bond direction. Therefore, the first SNP sample crystal was prepared with its c axis parallel to the cylinder axis. This ensured that the poles of the N0 and N1 EFG tensors could be rotated with our NMR probe into an orientation parallel to the applied field. Consequently, the cylinder axis of the

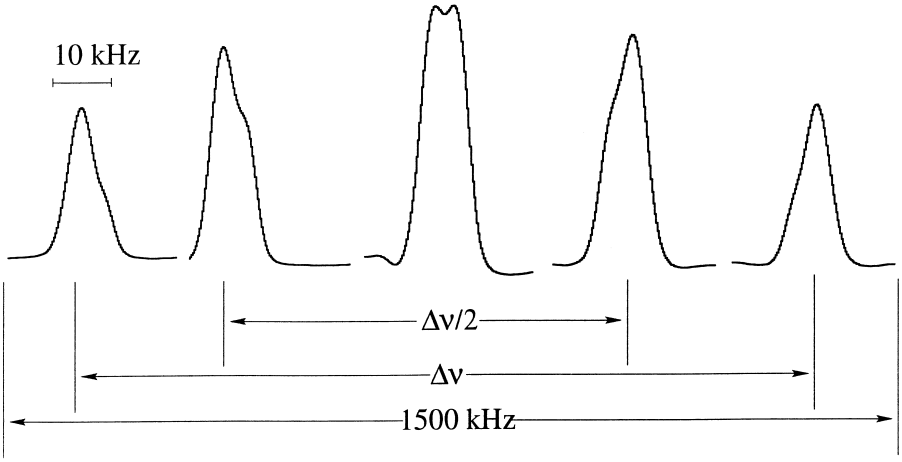

FIG. 3. ^{27}Al NMR spectrum of corundum (B = 11 T) for a crystal orientation near the tensor pole. Only the five ^{27}Al lines are shown, because their widths are much smaller than the width of the whole spectrum.

second NMR sample crystal was chosen to be perpendicular to the plane spanned by the C–N bonds of nitrogens N2 and N3. Because the tensor poles of the four inequivalent nitrogens in SNP do not lie in a plane, there is no crystal orientation which gives maximum NQR sensitivity for all nitrogens. For this reason, and for fully exploiting the available sample volume (38 cm^3) of the NQR spectrometer, we used a large (65 g) powder sample for the NQR measurements.

NMR

The NMR measurements were done with two Fourier transform spectrometers built around 6.3 and 11 T cryomagnets. In these fields, the Larmor frequencies of ^{27}Al and ^{14}N nuclei are, respectively, 69.89 and 122.03 MHz, and 19.37 and 33.82 MHz. Free-induction decays were excited with RF pulses of 1 μs duration, causing flips of the nuclear magnetization of roughly 10°. The spectral width of the excitation, about 1 MHz, is smaller than the full widths of the ^{14}N and ^{27}Al spectra in SNP and corundum. The ^{27}Al spectra of corundum were therefore recorded for each crystal orientation of interest in sections with a width of 500 kHz. Because of the large splittings of the various ^{14}N doublets in SNP, we found it more convenient to screen separately the ''northern'' and ''southern'' polar regions, corresponding to the high- and low-frequency lines near the tensor poles, of these resonances.

Figure 3 shows an 11 T ^{27}Al spectrum of corundum near the tensor pole. The shape of the satellites is conspicuously asymmetric. This results from the ^{27}Al–^{27}Al dipolar interactions (*18*) and provides welcome evidence that our spectral resolution is not limited by crystal imperfection, i.e., by a spread of EFGs. It is important to note that the true satellite position, i.e., that in the absence of dipolar interactions, is determined by the center of gravity of the satellite. This can be shown by calculating the first and second moments of the satellite lineshape and remembering that it is appropriate to truncate the dipolar Hamiltonian with respect to both the Zeeman and the quadrupolar interactions (*13*).

The dominant uncertainty in determining the center of gravity of the satellites results from the necessary phase correction of the FT spectra. Near the tensor pole, the satellites are far away from each other. It is therefore possible to phase each satellite separately using only a frequency-independent phase correction. According to tests with synthetic spectra, the usual judge for the correct phase, that is, the eye of the spectroscopist, leaves an uncertainty of about ±1.5°. We developed an interactive procedure that works for asymmetric lineshapes and improves the phase correction by such criteria as equality of steepness of the feet of the line and minimal dependence of the center of gravity from the width of the interval used for calculating this center. According to tests, this procedure allows us to reduce the uncertainty of the phase correction to ±0.5°. This corresponds to an uncertainty of ±0.08 kHz in the determination of the position of a satellite.

The ^{14}N NMR lines in SNP are symmetric, because their shape and width are due to ^{14}N dipolar coupling to the protons of the crystal water, i.e., to a *hetero*nuclear coupling. For phasing the spectra, we could therefore use an algorithm developed by Heuer for symmetric lines (*20*). The uncertainty left in determining the line positions was 0.02, 0.01, 0.02, and 0.05 kHz for the N0, N1, N2, and N3 lines, respectively. The differences result from the different widths of these lines.

The temperature dependence of the quadrupole coupling constant makes temperature and stability of temperature crucial considerations. We chose to carry out the corundum measurements at T = 303.2 K (30°C) and could keep this

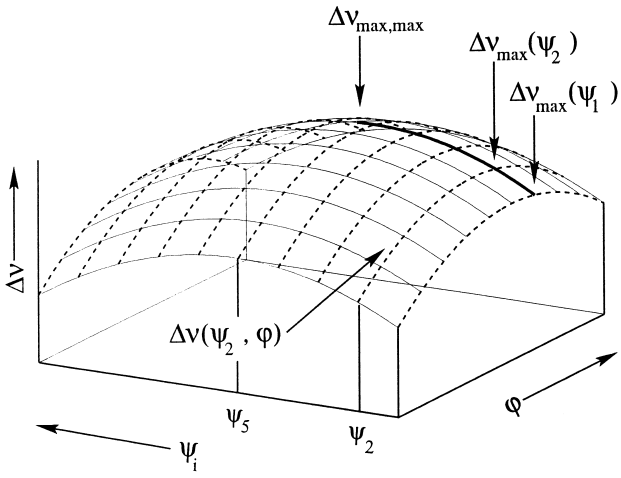

FIG. 4. Schematic representation of the nearly parabolic dependence of $\Delta\nu$ on the tilt angle ψ and on the rotation angle φ for a crystal orientation near the tensor pole.

temperature within ± 0.1 K. We used the same ITC-4 controller from Oxford Instruments and the same sensor, a 100 Ω Pt resistor, for both the 6.3 and 11 T measurements. Moreover, we measured, as mentioned in the Introduction, the temperature dependence of the splitting $\Delta\nu$ of the outer ^{27}Al satellites very close to the tensor pole. The results, expressed in terms of the QCC, are shown in Fig. 1. In the range $300 < T < 306$ K, the temperature dependence of $\Delta\nu$ can be expressed by $\Delta\nu(T) = \Delta\nu(303\ \mathrm{K}) + \alpha(T - 303\ \mathrm{K})$ with $\alpha = 0.03$ kHz/K.

For the ^{14}N measurements in SNP we adjusted the temperature to $T = 295$ K, with a stability of ± 0.1 K. In the range $292 < T < 298$ K, the temperature coefficients α of the line splittings close to the tensor poles of the N0, N1, N2, and N3 nitrogens were measured and were found to be 0.45, 0.40, 0.15, and 0.30 kHz/K, respectively. As our error analysis will show, the instability of the temperature of ± 0.1 K is not the limiting uncertainty of both our ^{27}Al and ^{14}N measurements. In order to determine the QCCs of the ^{27}Al site in corundum and of the ^{14}N sites in SNP we measured, as explained under Phenomenology, the orientation dependence of the splitting $\Delta\nu$ of the outer ^{27}Al satellites and that of the positions of the high- and low-frequency lines of the ^{14}N doublets, on a narrow grid in the (ψ, φ) plane near the respective tensor pole. As Fig. 4 shows schematically, $\Delta\nu$ near the tensor pole depends parabolically on both the rotation angle φ and the tilt angle ψ. The sequence of taking and processing the data may be followed in Fig. 4. For the ^{27}Al nuclei in corundum, the maximum splitting of the outer satellites was determined by a two-step fitting procedure. First, for a fixed tilt angle ψ_1, spectra were recorded for seven rotation angles φ with increments $\Delta\varphi$ of 1°. A parabola was fitted to the set of splittings $\Delta\nu(\psi_1, \varphi)$, and the maximum $\Delta\nu_{\max}(\psi_1)$ was computed. This procedure was repeated for 16 tilt angles ψ_i, $i = 1, \ldots, 16$, in the range $-3° < \psi < +3°$. Again, a parabola was fitted to the maxima obtained $\Delta\nu_{\max}(\psi_i)$. The apex $\Delta\nu_{\max,\max}$ of this parabola corresponds to the absolute maximum of $\Delta\nu$. The QCC of the ^{27}Al nuclei in corundum is then given by $\mathrm{QCC_{Al}} = \frac{5}{3}\Delta\nu_{\max,\max}$. Figure 5 shows the parabolas fitted to the values of $\Delta\nu_{\max}(\psi_i)$ obtained from the 6.3 and 11 T ^{27}Al data. The QCCs we find are

$$\mathrm{QCC_{Al}}(\mathrm{B} = 6.3\ \mathrm{T}) = 2403.10 \pm 0.15\ \mathrm{kHz}$$

and

$$\mathrm{QCC_{Al}}(\mathrm{B} = 11\ \mathrm{T}) = 2403.10 \pm 0.20\ \mathrm{kHz}$$

at T = 30°C. The errors will be discussed below.

For the ^{14}N sites in SNP, the procedure was the same except that the positions of the high- and low-frequency lines were measured and fitted separately, giving the ''north'' and

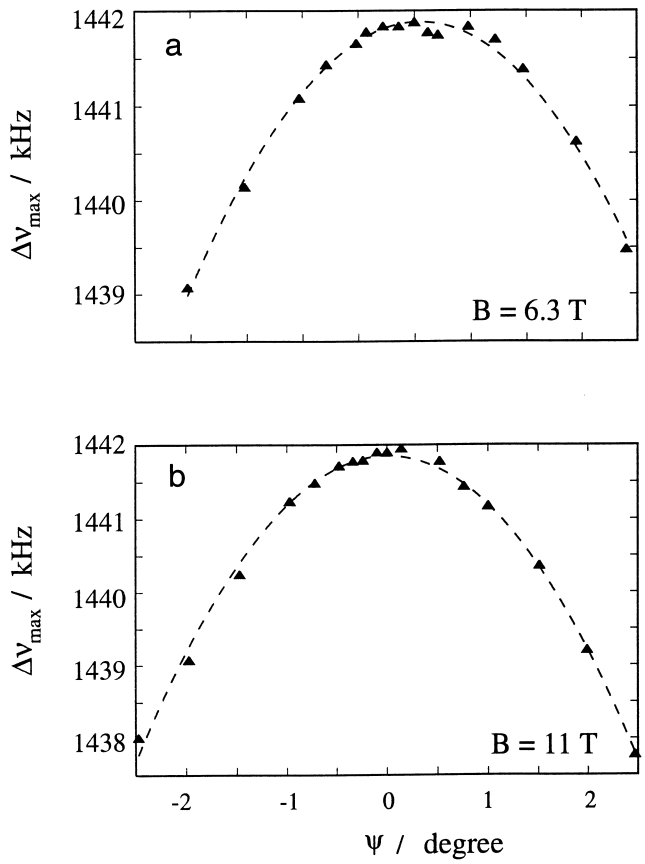

FIG. 5. $\Delta\nu_{\max}(\psi_i)$ plotted versus the tilt angle ψ for the outer satellite splitting of the ^{27}Al NMR lines in corundum in fields of 6.3 T (a) and 11 T (b). The parabolas fitted to the experimental values are also shown; their apexes give $\Delta\nu_{\max,\max}$.

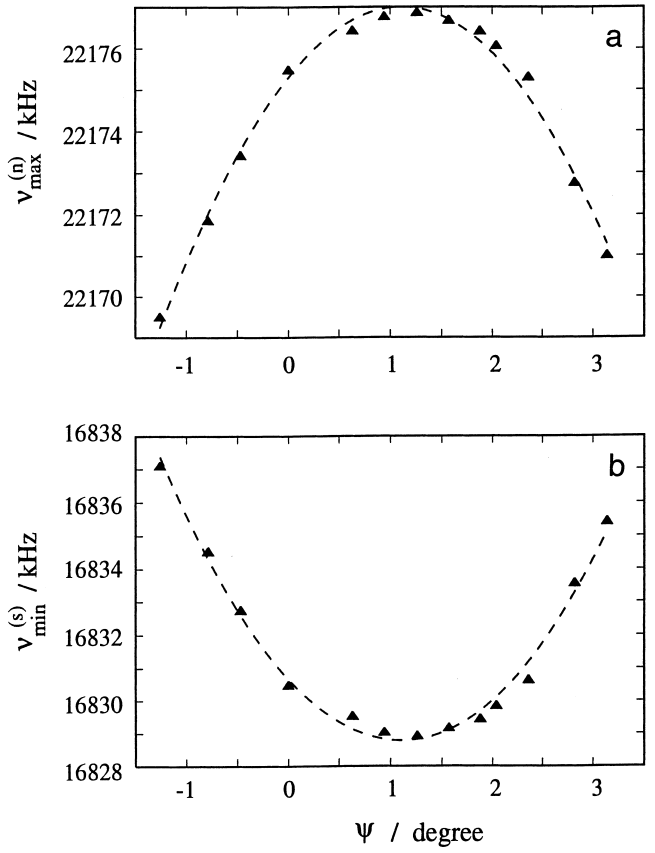

FIG. 6. $\nu^{(n)}_{max}(\psi_i)$ (a) and $\nu^{(s)}_{min}(\psi_i)$ (b) of the ^{14}N doublet for the N1 site in SNP, measured at $B = 6.3$ T and plotted versus the tilt angle ψ. The parabolas fitted to the experimental values are also shown; their apexes give $\nu^{(n)}_{max,max}$ and $\nu^{(s)}_{min,min}$, respectively.

''south pole'' frequencies $\nu^{(n)}_{max,max}$ and $\nu^{(s)}_{min,min}$. The QCC of an ^{14}N nucleus is

$$QCC = \tfrac{2}{3}\Delta\nu_{max,max} = \tfrac{2}{3}(\nu^{(n)}_{max,max} - \nu^{(s)}_{min,min}).$$

As an example we show in Fig. 6 the parabolas fitted to the values $\nu^{(n)}_{max}(\psi_i)$ and $\nu^{(s)}_{min}(\psi_i)$ of the N1 site in SNP at $B = 6.3$ T. The QCCs of all four distinct nitrogens in SNP obtained in this way for $B = 11$ and 6.3 T are listed in columns 1 and 2 of Table 2.

The experimental error of $\Delta\nu_{max,max}$, and that of QCC, depends on the errors of the measured line positions and of the orientation of the crystal. The former is dominated, as mentioned above, by the uncertainty of the phase correction and includes the error due to the temperature instability. All systematic errors such as the uncertainty of the synthesizer frequency and of the digitization rate of the analog-to-digital converter are negligibly small. The orientation error is minimized by the measurement and fitting procedure itself, which renders the result independent of any *absolute* orientation of the crystal. Nevertheless, an orientation uncertainty remains because of the limited precision of setting the increments $\Delta\varphi$ and $\Delta\psi$ of the rotation and tilt angles.

An estimate of the precision of our ^{27}Al NMR data is obtained by considering the root-mean-square deviation

$$\sigma = \left[\frac{\sum_{i=1}^{n}[\Delta\nu^{exptl}_{max}(\psi_i) - \Delta\nu^{fit}_{max}(\psi_i)]^2}{(n-2)}\right]^{1/2} \quad [10]$$

of the experimental data in Fig. 5 from the respective fitting curves. The denominator $(n - 2)$ takes into account that two variables, $\Delta\nu^{exptl}_{max}(\psi_i)$ and ψ_i itself, are prone to errors. The values of σ obtained in this way for the 6.3 and 11 T ^{27}Al data, multiplied by $\frac{5}{3}$ for the conversion of $\Delta\nu_{max,max}$ into QQC_{Al}, are the error limits quoted above for QCC_{Al} ($B = 6.3$ T) and $QQC_{Al}(B = 11$ T).

The error limits of the QCCs of the ^{14}N sites N0, . . . , N3 in SNP at 6.3 and 11 T were estimated analogously. While the first fit of the parabola to the ^{14}N line positions $\nu^{(n)}(\psi_i, \varphi)$ and $\nu^{(s)}(\psi_i, \varphi)$ indicated only statistical errors with average standard deviations as small as 0.05 kHz, it is obvious from Fig. 6 that the values $\nu^{(n)}_{max}(\psi_i)$ and $\nu^{(s)}_{min}(\psi_i)$ are not distributed purely statistically around the respective fitting curves. This is indicative of some hysteresis in the tilt mechanism of our probe which had not come to light during the less critical ^{27}Al measurements. In SNP, however, where the resonances are symmetric, narrower, and more widely split than in corundum, this hysteresis is the dominating error source.

NQR

^{27}Al in Corundum. Because the ^{27}Al EFG in corundum must be axially symmetric the NQR spectrum consists of two transitions $\nu_{\pm(1/2\leftrightarrow 3/2)}$ and $\nu_{\pm(3/2\leftrightarrow 5/2)}$ with frequencies ν_1 and $\nu_2 = 2\nu_1$. For determining QCC_{Al} in corundum in the absence of a magnetic field, it is thus sufficient to measure ν_2 which is related to $QCC_{Al}(B = 0)$ by

TABLE 2

The Quadrupole Coupling Constants of the Four Distinct Nitrogens in SNP, $Na_2[Fe(CN)_5NO] \cdot 2H_2O$, at 298 K, Obtained in Fields of 11 T and 6.3 T and in the Absence of an Applied Magnetic Field

Site	QCC (kHz) $B = 11$ T	QCC (kHz) $B = 6.3$ T	QCC (kHz) $B = 0$
N0	2233.99 ± 0.17	2233.92 ± 0.16	2233.97 ± 0.10
N1	3565.53 ± 0.30	3565.48 ± 0.32	3565.23 ± 0.15
N2	3512.87 ± 0.18	3512.75 ± 0.20	3513.01 ± 0.11
N3	3654.64 ± 0.24	3654.52 ± 0.31	3654.85 ± 0.13

Note. The labeling of the sites follows Fig. 2.

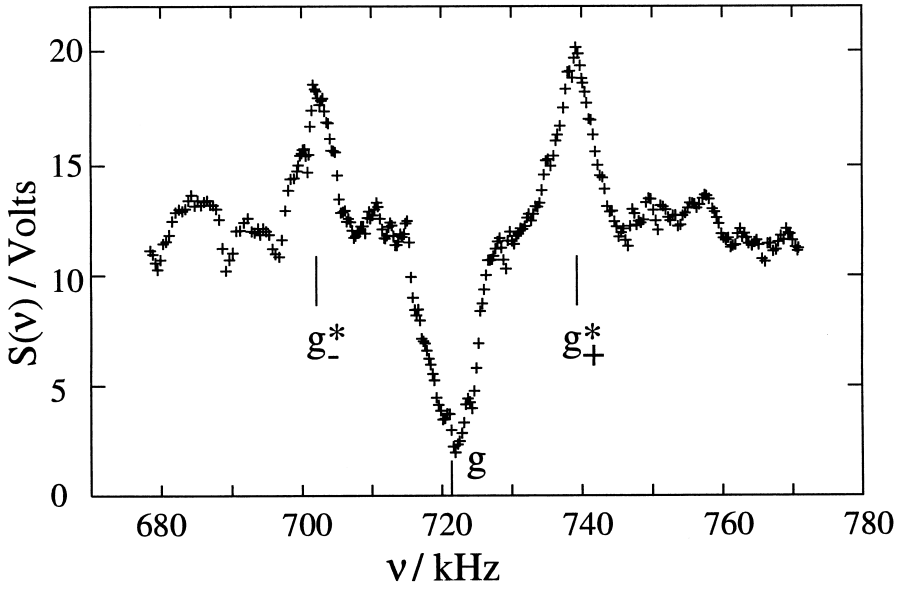

FIG. 7. Zeeman-modulated NQR spectrum of the $\nu_{\pm 5/2 \leftrightarrow \pm 3/2}$ transition in corundum. The center of gravity of the line $g(\nu)$ gives the transition frequency directly. The lines $g^*_{\mp}(\nu)$ and $g^*_{\pm}(\nu)$ arise from the Zeeman modulation; the average of their centers of gravity again gives the pure NQR transition frequency.

$$\nu_2 = \tfrac{3}{10}\mathrm{QCC}_{\mathrm{Al}}(B = 0). \qquad [11]$$

Because any magnetic field dependence of $\mathrm{QCC}_{\mathrm{Al}}$ will be extremely small, we can predict from our NMR results that ν_2 will be very close to 720.9 kHz. This knowledge is highly valuable in the search for the ^{27}Al NQR in corundum.

To date, the best apparatus for detecting such a low-frequency NQR transition is probably the Robinson-oscillator CW NQR spectrometer of P. J. Bray with the option of applying Zeeman modulation (*19*). Professor Bray was kind enough to make available this spectrometer to us.

The baseline-corrected ^{27}Al spectrum of the ν_2 transition, recorded at $T = 30$°C, is shown in Fig. 7. The $g^*_{\mp}(\nu)$ and $g^*_{\pm}(\nu)$ lines in this figure are due to the Zeeman modulation with $|\mathbf{B}_{\mathrm{mod}}| = 2.4$ mT, the inverted line $g(\nu)$ gives the ν_2 transition directly. The centers of gravity $\nu^*_{\mp}$, $\nu^*_{\pm}$ and ν_2 of these lines are

$$\nu_2 = (720.97 \pm 0.9)\ \mathrm{kHz}$$

$$\nu^*_{\mp} = (702.45 \pm 1.0)\ \mathrm{kHz}$$

$$\nu^*_{\pm} = (738.59 \pm 0.7)\ \mathrm{kHz}.$$

The error limits were estimated from the dependence of these numbers on the integration limits used for calculating the centers of gravity. All systematic errors related to the apparatus (e.g., line distortion by the low-pass filter in the lock-in amplifier, frequency measurement, variation of the frequency sweep rate $d\nu/dt$ and temperature) were negligibly small compared with that associated with the determination of the centers of gravity of the noisy lines in Fig. 7.

According to the first-order perturbation treatment of the Zeeman modulation, we have

$$1/2(\nu^*_{\mp} + \nu^*_{\pm}) = \nu_2. \qquad [12]$$

The experimental number for this indirect value of ν_2 is (720.52 ± 0.6) kHz. Combining the direct and indirect values of ν_2, we obtain

$$\nu_{2,\mathrm{exptl}} = (720.70 \pm 0.5)\ \mathrm{kHz}$$

and

$$\mathrm{QCC}_{\mathrm{Al}}(B = 0) = (2402.5 \pm 1.7)\ \mathrm{kHz}$$

at $T = 30$°C. We thus find that the quadrupole coupling constant of the ^{27}Al nuclei in corundum, measured in the absence of an applied field, agrees within the error limits with the corresponding values measured at 6.3 and 11 T.

The NQR measurement of $\mathrm{QCC}_{\mathrm{Al}}$ is considerably less precise than the NMR measurements. The reason is twofold: first, the conversion factor from the directly measured quantities, ν_2 and $\Delta\nu_{\mathrm{max,max}}$, to $\mathrm{QCC}_{\mathrm{Al}}$ is different, 10/3 in the former, 5/3 in the latter case. Second, the signal-to-noise ratio is much better in the NMR than in the NQR spectra, whereas the NQR and NMR linewidths are roughly the same.

^{14}N in SNP. For each of the four independent ^{14}N nuclei k in SNP, there are three NQR transitions, which occur at $\nu_{\pm}^{(k)} = \frac{3}{4}QCC_k(B = 0)[1 \pm \eta_k/3]$ and $\nu_0^k = \frac{1}{2}\eta_k QCC_k(B = 0)$. Because we had already measured the quadrupole coupling constants QCC_k at $B = 6.3$ and 11 T, and because we know the asymmetry parameters η_k from (*4*), we had, prior to the NQR measurements proper, an excellent starting knowledge of the frequencies $\nu_{\pm}^{(k)}$ and $\nu_0^{(k)}$. All the $\nu_0^{(k)}$ are lower than 100 kHz, and we made no effort to detect these transitions. Their knowledge is not necessary for our present purpose. To detect the $\nu_{\pm}^{(k)}$ transitions, which occur in the frequency range of $1.6 \cdots 2.8$ MHz, we used a Matec FT NQR spectrometer. It was driven with the same frequency synthesizer that was used for the NMR measurements. The sample temperature was also measured and controlled by the same sensor and controller. This ensured that there were no systematic frequency and temperature differences between the NMR and NQR measurements.

Each of the eight transitions $\nu_{\pm}^{(k)}$ was detected separately with a $\pi/2$—τ—π—τ—echo sequence. The width of the $\pi/2$ pulse was 5 μs. The second half of the echo was accumulated between 1000 and 2000 times, using a repetition time of 1 s and a sampling rate of 50 μs^{-1}, and Fourier transformed. The prior knowledge of the frequencies $\nu_{\pm}^{(k)}$ was sufficient, on the one hand, to make sure that a selected transition fell well within the spectral window of 10 kHz and, on the other hand, to safely assign all the transitions. In Fig. 8, we reproduce the NQR spectra of the N1 . . . N3 nitrogens to convey an impression of their quality. To determine the centers of gravity of the recorded lines, we fitted gaussians to the experimental data. As stated above, the necessary phase correction step in the data analysis introduces the dominant uncertainty into the determination of the centers of gravity of the recorded lines and therefore into the measurement of the quadrupole coupling constants $QCC_k(B = 0)$. These quadrupole coupling constants are listed together with the estimated error limits in the third column of Table 2.

Note that our ^{14}N NQR data are more precise than our ^{14}N NMR data, but the opposite is true of our ^{27}Al data. The reason for this difference is twofold. First, the ^{14}N NQR frequencies in SNP are much larger and are therefore detectable with a better signal/noise ratio than the ^{27}Al NQR frequency in corundum. Second, the ^{14}N NMR and NQR resonances in SNP are much narrower than their ^{27}Al counterparts, as shown in Figs. 3, 7, and 8. The consequence is that the imperfections of the tilt mechanism of our probe, which had not limited the precision of our ^{27}Al NMR results, was the dominant error source of our ^{14}N NMR measurements, whereas the ^{14}N NQR measurements fully profited from the narrow resonances.

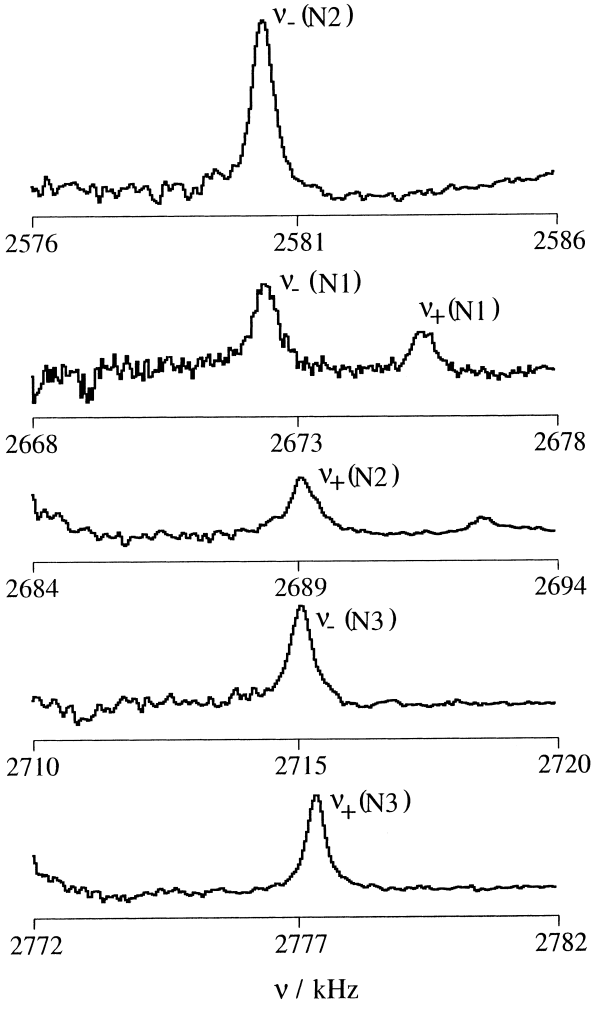

FIG. 8. ^{14}N NQR spectra of SNP in the region of the C–N resonances. The spectra were obtained by Fourier transforming the second half of an echo signal. Each spectrum corresponds to a separate setting of the spectrometer frequency indicated by the frequency on the left side of the spectrum. The ν_+ and ν_- resonances of the N–O nitrogen occur at 1692.28 and 1658.67 kHz.

DISCUSSION AND CONCLUSIONS

By applying special NMR procedures in fields of 6.3 and 11 T, we succeeded in determining the quadrupole coupling constant of the ^{27}Al nuclei in corundum with a relative error $\delta QCC/QCC$ of only 6×10^{-5}, and the quadrupole coupling constants of the four distinct ^{14}N nuclei in SNP with an average relative error of 7×10^{-5}. Our results from pure NQR measurements, somewhat less precise for the ^{27}Al nuclei in corundum but more precise for the ^{14}N nuclei in SNP, fully agree with our numbers derived from NMR. We conclude that, to a precision of 6×10^{-5}, a magnetic field dependence of quadrupole coupling constants, that is, an effect in the sense of this work, does not exist in corundum and in SNP. Our considerations about orbital quenching and time-reversal symmetry suggest that this statement can safely be generalized to the nuclear quadrupole moment–electric-field gradient interaction in all *diamagnetic* compounds. To be cautious, we should add that this statement

should be correct, provided that considerations are restricted to magnetic fields that are currently available for NMR experiments, that is, to fields of up to at least 20 T. We note that there are places in the universe where very much higher fields exist, and, even on this planet, theorists are by no means restricted to thinking only of fields up to 20 T.

Our considerations suggest, on the other hand, that an effect on the level of precision achieved in this work should exist in materials with *ordered electron* spins, that is, in ferromagnetic and antiferromagnetic compounds. A literature survey of magnetic resonance in ferromagnetic and antiferromagnetic compounds convinced us, however, that it is not possible at the present time to measure the field dependence of quadrupole coupling constants in such systems with the same precision as we achieved here in corundum and SNP. One of the starting points of the experimental part of this work was the discrepancy between the 8.4 T ^{14}N NMR data of SNP reported by Gross *et al.* (*4*) and the ^{14}N NQR data reported by Murgich *et al.* (*5*). The NQR as well as the NMR data of this work, obtained at $T = 298$ K, agree within 3–5 kHz with the NQR data of the NQR frequency-vs-temperature curves in Fig. 2 of Ref. (*5*). A shift of 9 K in the calibration of our thermometer relative to that of Murgich's would reduce all the remaining differences to below 1 kHz. This stresses again the importance of carefully measuring (and reporting) the temperature in all work on quadrupole coupling constants and quadrupole coupling tensors. The absolute uncertainty of our temperature measurements is certainly much smaller than 9 K. Comparing the results of this work with those of Gross *et al.* (*4*) leads to the conclusion that the analysis of the rotation patterns of quadrupole splittings in the latter work, when expressed in terms of QCCs, entailed errors as large as 24 kHz, as indicated by the entries for N2 in Table 2 compared to those in column 1 of Table 1. Fairness requires, however, to say that the measurement of the room temperature ^{14}N QCCs in SNP was only a side aspect of the work of Gross. Its primary concern was the elucidation of the fascinating new metastable electronic state in SNP with virtually infinite lifetime at $T < 100$ K (*21*).

ACKNOWLEDGMENTS

In 1991, Rex Gerald II, then a Ph.D. student of C. J. Jameson in Chicago, initiated the present study by confronting us with the argument that the magnetic-field-induced modification of the electronic wavefunction, which gives rise to chemical shifts, must also lead to a modification of the EFG. We are grateful to Professor S. Haussühl from the University of Cologne for giving us three large oriented crystals of SNP. During his stay in Providence, RI, B.F. enjoyed the warm hospitality of Professor P. J. Bray. We appreciate and acknowledge the help of G. Mozjouhine from the University of Kaliningrad in the ^{14}N NMR portion of this work.

REFERENCES

1. C. Kittel, ''Introduction to Solid State Physics,'' 2nd ed., Chap. 15, Wiley, New York, 1957.
2. C. P. Slichter, ''Principles of Magnetic Resonance,'' Chap. 4.3 Harper & Row, New York, and Weatherhill, Tokyo, 1963.
3. P. Gutsche, Diploma thesis, University of Heidelberg, 1996.
4. D. Gross, N. Pislewski, U. Haeberlen, and K. H. Hausser, *J. Magn. Reson.* **54,** 236 (1983).
5. J. Murgich and R. Ambrosetti, *J. Magn. Reson.* **74,** 344 (1987).
6. R. V. Pound, *Phys. Rev.* **79,** 685 (1950).
7. J. Chang, C. Connor, E. L. Hahn, H. Huber, and A. Pines, *J. Magn. Reson.* **82,** 387 (1989).
8. H. J. Jakobsen, J. Skibsted, H. Bildsoe, and N. C. Nielsen, *J. Magn. Reson.* **85,** 173 (1989).
9. S. J. Gravina and P. J. Bray, *J. Magn. Reson.* **89,** 515 (1990).
10. R. E. Newnham, Y. M. De Haan, Z. Kristallogr. **117,** 235 (1962).
11. B. Tesche, H. Zimmermann, R. Poupko, and U. Haeberlen, *J. Magn. Reson. A* **104,** 68 (1993).
12. S. Malinowski, *Phys. Rev. B* **49,** 8 (1994).
13. B. Filsinger, Dissertation, University of Heidelberg, 1994.
14. K. Schmidt-Rohr and H. W. Spiess, ''Multidimensional Solid-State NMR and Polymers,'' Academic Press, London, 1994.
15. S. Haussühl, ''Kristallphysik,'' Physik Verlag, Weinheim, 1983.
16. U. Haeberlen, ''High Resolution NMR in Solids. Selective Averaging,'' Academic Press, New York, 1976.
17. F. Bottomley and P. S. White, *Acta Crystallogr. Sect. B,* **35,** 2193 (1979).
18. A. H. Silver, T. Kushida, and J. Lambe, *Phys. Rev.* **125,** 1147 (1961).
19. F. N. H. Robinson, *J. Sci. Instrum.* **36,** 481 (1959).
20. A. Heuer, *J. Magn. Reson.* **91,** 241 (1991).
21. U. Hauser, V. Oestreich, and H. D. Rohrweck, *Z. Phys. A* **280,** 17 (1977).